Published October 25, 2010

Integrated biochemical and mechanical signals regulate multifaceted human embryonic stem cell functions

Dong Li,[1,2] Jiaxi Zhou,[1,2] Lu Wang,[1,2] Myung Eun Shin,[1,2] Pei Su,[1,2] Xiaohua Lei,[5] Haibin Kuang,[5] Weixiang Guo,[5] Hong Yang,[1,2] Linzhao Cheng,[6] Tetsuya S. Tanaka,[1,3] Deborah E. Leckband,[4] Albert B. Reynolds,[7] Enkui Duan,[5] and Fei Wang[1,2]

[1]Institute for Genomic Biology, [2]Department of Cell and Developmental Biology, [3]Department of Animal Sciences, and [4]Department of Chemical and Molecular Engineering, University of Illinois at Urbana-Champaign, Urbana, IL 61801
[5]State Key Laboratory of Reproductive Biology, Institute of Zoology, Chinese Academy of Science, Beijing 100101, China
[6]Stem Cell Program, Institute for Cell Engineering, School of Medicine, Johns Hopkins University, Baltimore, MD 21205
[7]Department of Cancer Biology, Vanderbilt University, Nashville, TN 37232

Human embryonic stem cells (ESCs [hESCs]) proliferate as colonies wherein individual cells are strongly adhered to one another. This architecture is linked to hESC self-renewal, pluripotency, and survival and depends on epithelial cadherin (E-cadherin), NMMIIA (nonmuscle myosin IIA), and p120-catenin. E-cadherin and p120-catenin work within a positive feedback loop that promotes localized accumulation of E-cadherin at intercellular junctions. NMMIIA stabilizes p120-catenin protein and controls E-cadherin–mediated intercellular adhesion. Perturbations of this signaling network disrupt colony formation, destabilize the transcriptional regulatory circuitry for pluripotency, and impair long-term survival of hESCs. Furthermore, depletion of E-cadherin markedly reduces the efficiency of reprogramming of human somatic cells to an ESC-like state. The feedback regulation and mechanical–biochemical integration provide mechanistic insights for the regulation of intercellular adhesion and cellular architecture in hESCs during long-term self-renewal. Our findings also contribute to the understanding of microenvironmental regulation of hESC identity and somatic reprogramming.

Introduction

Human embryonic stem cells (ESCs [hESCs]), derived from the inner cell mass of blastocyst-stage human embryos, can self-renew in culture indefinitely and have the remarkable potential to develop into nearly all differentiated cell types (Thomson et al., 1998), allowing them to be used for biomedical research, drug discovery, and cell-based therapies (Daley and Scadden, 2008; Rossant, 2008). hESC long-term self-renewal requires cell proliferation and survival with continuous repression of differentiation. Recent studies have revealed some important molecular elements that support hESC long-term undifferentiated growth and survival. Extrinsic factors such as basic FGF (bFGF; Thomson et al., 1998; Levenstein et al., 2006), TGF-β (Xu et al., 2008), and insulin-like growth factor 1 (Bendall et al., 2007) are required for stability of a network of transcription factors including OCT-4, NANOG, and SOX2, which function in concert to positively regulate target genes necessary for pluripotency and repress a variety of lineage specification factors (Jaenisch and Young, 2008). Receptor tyrosine kinases, including ERBB2 and insulin-like growth factor 1 receptor (Wang et al., 2007), are necessary for hESC proliferation and survival. The signals from the extrinsic factors are integrated by intracellular molecules, such as mammalian target of rapamycin (mTOR; Zhou et al., 2009), to repress differentiation activities and/or

D. Li and J. Zhou contributed equally to this paper.

Correspondence to Fei Wang: feiwang@life.uiuc.edu

Abbreviations used in this paper: bFGF, basic FGF; E-cadherin, epithelial cadherin; ESC, embryonic stem cell; hE/Fc, E-cadherin/Fc proteins; hESC, human ESC; hiPSC, human iPSC; iPSC, induced pluripotent stem cell; MEF, mouse embryonic fibroblast; mESC, mouse ESC; mTOR, mammalian target of rapamycin.

Supplemental Material can be found at:
http://jcb.rupress.org/content/suppl/2010/10/25/jcb.201006094.DC1.html

The Rockefeller University Press $30.00
J. Cell Biol. Vol. 191 No. 3 631–644
www.jcb.org/cgi/doi/10.1083/jcb.201006094

Published October 25, 2010

promote proliferation and survival of hESCs. Despite the understanding of hESC regulation by soluble factors, little is known mechanistically about how other microenvironmental factors including cell–cell and cell–ECM interactions control hESC functions.

In this study, we investigate a distinctive feature of hESCs. Like ESCs established from other species, hESCs proliferate in culture as tight and compact colonies, wherein cells are associated strongly with one another (Thomson et al., 1998). The compact structure of hESCs appears integral to the normal functions of hESCs. Perturbations of hESC pluripotency as the result of the removal or inhibition of key extrinsic factors, intracellular signaling molecules, and transcription factors are associated with profound changes in cell and colony morphologies (Levenstein et al., 2006; Okita and Yamanaka, 2006; Zhou et al., 2009). One of the changes is loss of colony integrity and disruption of proper intercellular interactions. Therefore, maintenance of cellular association and colony integrity is a widely accepted indicator of the ESC state. Accordingly, in the recent derivation of induced pluripotent stem cells (iPSCs) from somatic cells, development of compact colonies with tight cellular association has been used as a simple and reliable readout for conversion of non-ESCs to an ESC-like state (Takahashi and Yamanaka, 2006; Takahashi et al., 2007; Yu et al., 2007; Park et al., 2008). Despite the evident role of cellular association in regulating hESC functions, the mechanisms and molecular connections to pluripotency remain largely undefined.

Cadherins (calcium-dependant adhesion molecules) are a class of type 1 transmembrane proteins that play important roles in intercellular cell adhesion (Takeichi, 1995). In particular, epithelial cadherin (E-cadherin) plays a pivotal role in tissue morphogenesis, development, tumorigenesis, and signal transduction (Gumbiner, 2005). E-cadherin is highly expressed in hESCs, and inhibition of E-cadherin function impairs cell survival (Li et al., 2010; Xu et al., 2010). β-Catenin and p120-catenin bind the cytoplasmic domain of E-cadherin and are critical regulators of E-cadherin functions (Cowin and Burke, 1996; Davis et al., 2003; Xiao et al., 2003). α-Catenin, an actin-binding protein, regulates interaction of the E-cadherin–β-catenin complex with the actin cytoskeleton (Drees et al., 2005; Yamada et al., 2005). α-, β-, and p120-catenin have established roles in early development; ablation or depletion of these molecules caused embryonic lethality in mice and other animals (Haegel et al., 1995; Torres et al., 1997; Fang et al., 2004; unpublished data). The roles of α-, β-, and p120-catenin in regulating hESC adhesion and pluripotency have not been explored. This can be largely attributed to the difficulties associated with genetic manipulations of hESCs, including the use of RNAi-mediated knockdown of genes of interest.

In this study, we identified a highly integrated signaling network that controls intercellular adhesion in hESCs. This network contains NMMIIA (nonmuscle myosin IIA), E-cadherin, and p120-catenin and is essential for colony formation, stability of the transcriptional regulatory circuitry for pluripotency, and long-term survival of hESCs.

Results

Inhibition of NMMII causes profound defects in hESCs

To identify the regulatory components of pluripotency in hESCs, we screened a collection of pharmacological inhibitors against kinases and other signaling molecules. To eliminate indirect effects of feeders on hESCs, we used feeder-free culture conditions, under which untreated control cells grew as compact and tight colonies with well-defined edges (Fig. 1 A; Xu et al., 2001). We passaged hESCs as small cell clusters, a condition known to improve cell survival. This screening effort led us to identify mTOR as a central regulator of hESC pluripotency (Zhou et al., 2009). With this screen, we also found that treatment of cells with blebbistatin, a highly specific inhibitor of NMMII (Straight et al., 2003), induced profound morphological changes in H9 hESCs. Blebbistatin-treated cells formed poorly developed colonies in which a significant fraction of cells were dissociated from one another and spread out as single cells (Fig. 1 A; several representative cell morphologies are shown in Fig. S1 A). The effect of blebbistatin on colony formation was dose dependent, with an inhibitory concentration for 50% inhibition (IC50; disruption of ∼50% of colonies) of ∼4 μM, which is close to the reported IC50 value for inhibiting ATPase activity of myosin II (∼2 μM; Straight et al., 2003). Exposure of cells to 10 μM blebbistatin caused the poorly aggregated colonies to increase from 9 (for control cells) to 82% (Table S1). This dose was used for the rest of the experiments.

Disruption of colony integrity is often associated with altered expression of pluripotency markers. Indeed, blebbistatin treatment reduced the activity of AP (an ESC marker) and the levels of SOX2, NANOG, and OCT-4 proteins in H9 cells (Fig. 1, B and C; and Fig. S1 B; quantification of SOX2, NANOG, and OCT-4 levels is shown in Table S1). SOX2, NANOG, and OCT-4 are components of the core transcriptional regulatory circuitry for pluripotency (Jaenisch and Young, 2008) and have also been used to derive human and mouse iPSCs (Takahashi and Yamanaka, 2006; Takahashi et al., 2007; Yu et al., 2007; Park et al., 2008). Interestingly, the mRNA levels of *POU5F1* (the gene encoding OCT-4), *SOX2*, and *NANOG* decreased only slightly after blebbistatin treatment (Fig. S1 C), indicating that the regulation largely occurred posttranscriptionally. Blebbistatin's effect on the pluripotency factors was also observed in H1 hESCs (Thomson et al., 1998), a human iPSC (hiPSC) line MMW2 (Mali et al., 2010) and W4/129 mouse ESCs (mESCs; Fig. S1, D–F), implying a conserved function of NMMII in pluripotent stem cells. Furthermore, although blebbistatin treatment for 5 d exerted little effect (blebbistatin-treated cells, 7 ± 4%; vs. control cells, 5 ± 3%), long-term treatment (>7 d) caused increased apoptosis in hESCs (17 ± 7%; vs. control cells on day 8, 6 ± 3%; $P < 0.001$). The increase in apoptosis was likely the result of the gradual loss of cellular association after prolonged treatment. It is well known that cellular association is required for survival of hESCs (Watanabe et al., 2007).

To ask whether NMMII inhibition also impaired de novo colony formation in hESCs, we assessed the effects of blebbistatin on hESCs plated as single cells. Interestingly, blebbistatin

Published October 25, 2010

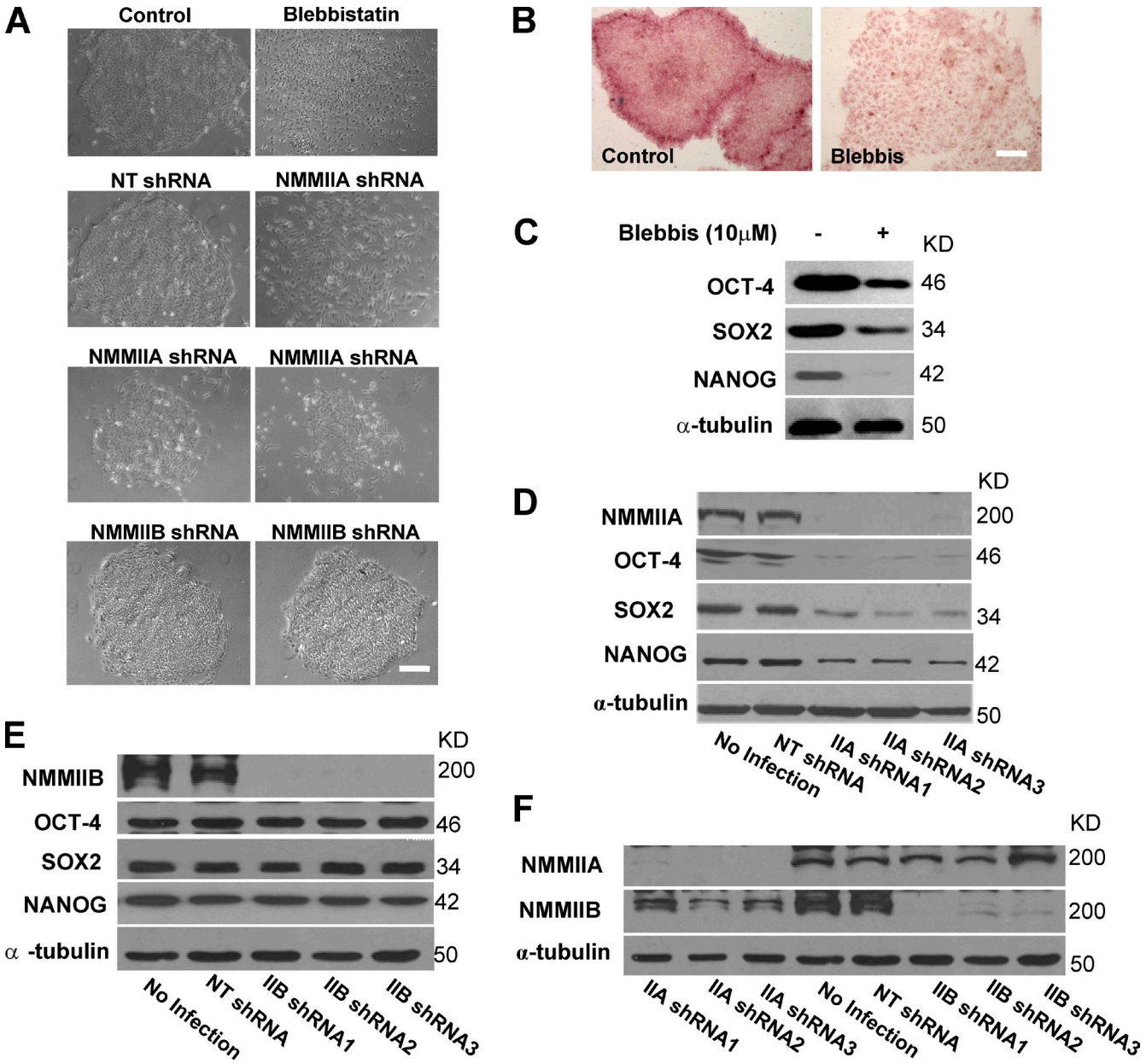

Figure 1. **NMMIIA but not NMMIIB is necessary for multifaceted hESC functions.** (A) Phase-contrast images of H9 cells cultured under feeder-free conditions with or without the following treatments: 10 μM blebbistatin (5 d), nontargeting shRNA (NT shRNA), NMMIIA, or NMMIIB shRNAs (4 d). (B) AP staining of H9 cells with or without 10 μM blebbistatin treatment (5 d). More images are shown in Fig. S1 A. (A and B) Bars, 100 μm. (C) Western blot analysis of OCT-4, SOX2, and NANOG proteins in H9 cells treated with or without 10 μM blebbistatin (5 d). A typical blot is shown, and quantification of blots from four separate experiments is shown in Table S1. α-Tubulin was a loading control. (D and E) Western blot analysis of NMMIIA/NMMIIB, OCT-4, SOX2, and NANOG proteins in H9 cells with or without NMMIIA/NMMIIB depletion (4 d). Three different shRNAs targeting NMMIIA (D) or NMMIIB (E) were used. Cells without lentiviral infection (no infection) or treated with nontargeting shRNA were used as negative controls. Quantifications of blots from four separate experiments for NMMIIA and NMMIIB depletion are shown in Table S1. Cells infected with nontargeting shRNA exhibited similar values to cells without infection. (F) Western blot analysis of NMMIIA or NMMIIB in H9 cells with NMMIIA or NMMIIB depletion, respectively.

treatment increased the number of surviving single cells (from ~7 to 35%) 24 h after plating (Fig. S1 G), which is consistent with a previous report that inhibition of ROCK or other components of the Rho–ROCK–NMMII cascade improved survival of dissociated hESCs (Watanabe et al., 2007; Xu et al., 2010). Under this condition, prolonged blebbistatin treatment markedly impaired colony formation and increased the colonies with poor cellular association to 86% (Fig. S1 G and not depicted). The treatment also reduced the levels of OCT-4, NANOG, and SOX2 proteins (Fig. S1 H). Thus, NMMII is necessary for stability of the OCT-4–SOX2–NANOG circuitry and colony formation in hESCs, regardless of whether they are plated as single cells or small clusters.

We next determined whether the changes induced by myosin II inhibition were reversible. To test this, we removed blebbistatin from cells after a 3-d treatment and allowed them to continue to grow for 3 d without blebbistatin. In a separate experiment, we incubated the cells with blebbistatin for 5 d,

Published October 25, 2010

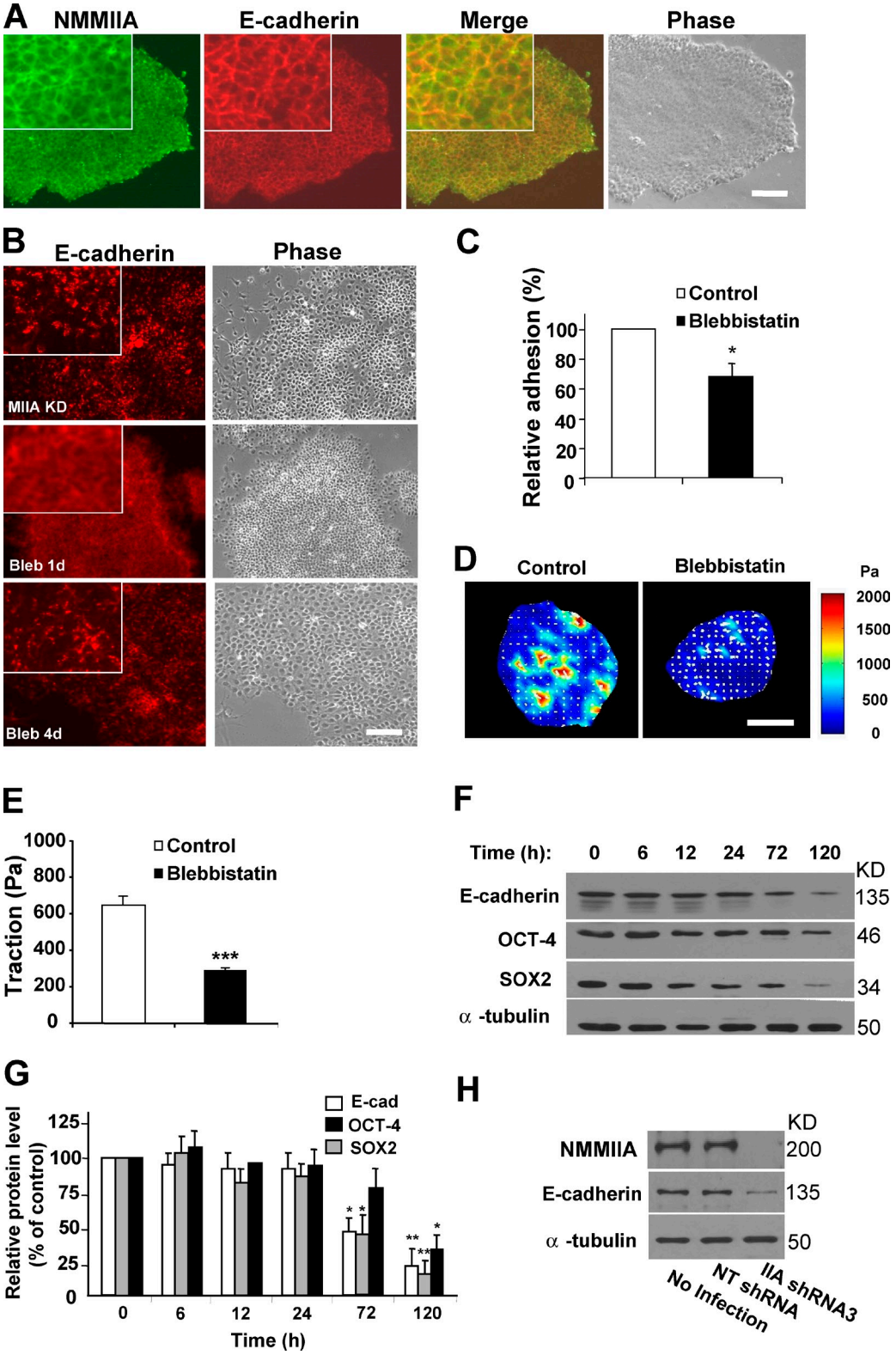

Figure 2. **NMMIIA modulates E-cadherin adhesion and protein expression in hESCs.** (A) Fluorescence and phase-contrast images of H9 cells stained with antibodies against NMMIIA and E-cadherin. (B) Immunofluorescence experiments of E-cadherin in H9 with NMMIIA depletion (for 4 d) or treated with 10 µM blebbistatin for 24 h or 4 d. Corresponding phase-contrast images of the cells are also shown. (A and B) Insets show fractions of fluorescence images at a higher magnification. Bars, 100 µm. (C) Relative cell adhesion to the E-cadherin substrate hE/Fc with or without 10 µM blebbistatin treatment (2 h). Values were normalized to the number (100%) of control cells. Results from five separate experiments are shown. Student's *t* tests compared data between the two experimental groups. (D) Representative traction maps for hESCs plated on elastic polyacrylamide gels coated with hE/Fc with or without blebbistatin treatment. The pseudocolor bar represents tractions. Bar, 5 µm. (E) Mean tractions in control cells and cells with blebbistatin treatment. Cells were analyzed 1 h after being plated on elastic polyacrylamide gel coated with hE/Fc. A customized MATLAB program (MathWorks) was used to calculate the traction values. (F) Western blot analysis of E-cadherin, OCT-4, and SOX2 proteins in H9 cells treated or not with 10 µM blebbistatin for various times.

Published October 25, 2010

replated the cells, and allowed them to grow for 5 d in the absence of blebbistatin. Under both conditions, cells with prior treatment were able to resume their original cellular morphology and rescue the levels of pluripotency proteins when cultured without blebbistatin (Fig. S1, I and J; and not depicted).

Disruption of the OCT-4–NANOG–SOX2 circuitry often causes differentiation activities in hESCs (Jaenisch and Young, 2008), leading us to examine the expression of lineage-specific differentiation markers in blebbistatin-treated cells. Blebbistatin treatment for 5 d enhanced expression of lamin A/C (Fig. S1 K), which was reportedly activated upon differentiation of mouse and hESCs (Constantinescu et al., 2006) but only induced slight up-regulation of *NEUROD1* (ectoderm), *MESP1*, *MIXL1* (mesoderm), *GATA4*, *GATA6* (endoderm), *CDX2*, and *CGB7* (trophoectoderm) (Fig. S1 L and not depicted).

Depletion of NMMIIA but not NMMIIB mimics blebbistatin treatment

NMMIIs are actin-binding proteins that regulate the contractile functions in cells. Of the three different NMMII isoforms identified, two (NMMIIA and NMMIIB) are almost ubiquitously found in higher organisms and are essential for development. Deletion of NMMIIA or NMMIIB in mice leads to embryonic lethality (Tullio et al., 1997; Conti et al., 2004). However, NMMIIA knockout leads to lethality in periimplantation stage embryos, whereas NMMIIB-null mice die late in gestation. hESCs, like mESCs (Conti et al., 2004), express both NMMIIA and NMMIIB (Fig. 1, D and E). To verify the specificity of blebbistatin and identify the NMMII isoforms required for hESC colony integrity and stability of the transcriptional circuitry for pluripotency, we exploited RNAi-induced knockdown to deplete NMMIIA and NMMIIB in hESCs. By infecting the cells with shRNA-containing lentivirus followed by puromycin selection, we achieved consistent knockdown of genes of interest in hESCs (see following paragraphs; Fig. 1 D; the effect of OCT-4 knockdown is shown in Fig. S2, A and B). To ensure specificity, we used at least two shRNAs to deplete the same target genes. Depletion of NMMIIA for 4 d sharply increased the proportion of colonies with poor cellular association (from 11% for control cells to 78%; Fig. 1 A) and markedly down-regulated OCT-4, NANOG, and SOX2 proteins (Fig. 1 D; and quantifications are shown in Table S1), which is highly reminiscent of blebbistatin treatment. In addition, although short-term depletion (4 d) of NMMIIA caused little effects (control, 6 ± 4%; vs. NMMIIA depletion, 7 ± 3%), long-term depletion (>7 d) led to marked apoptosis in hESCs (NMMIIA-depleted cells, 32 ± 5%; nontargeting shRNA control cells on day 8, 7 ± 3%; $P < 0.001$). The elevated apoptosis in NMMIIA-depleted cells was preceded by a robust reduction in the c-Myc protein (see Fig. 3 F; unpublished data). c-Myc is a transcription factor and acts as a key regulator of cell growth and survival. In contrast, depletion of NMMIIB had little effect on the pluripotency factors, colony formation, and long-term cell survival (Fig. 1, A and E; Table S1; and not depicted). The shRNA sequences targeting NMMIIA or NMMIIB effectively depleted their respective targets in H9 cells, demonstrating high specificity of shRNAs (Fig. 1 F). These results suggest that NMMIIA but not NMMIIB is necessary for colony formation, stability of the OCT-4–NANOG–SOX2 circuitry, and long-term survival of hESCs. The requirement of NMMIIA for supporting the ESC state might explain in part the early developmental defects observed in NMMIIA-null mice.

NMMIIA modulates E-cadherin adhesion and protein expression in hESCs

We next assessed NMMIIA's subcellular localization in hESCs. Immunofluorescence of NMMIIA was mainly distributed at cell–cell junctions, colocalizing with the adhesion molecule E-cadherin (Fig. 2 A). This raises the possibility that NMMIIA might regulate intercellular junctions in hESCs. Consistent with this idea, NMMIIA depletion for 4 d markedly impaired the accumulation of E-cadherin at the junctional sites and caused it to distribute diffusely or in punctuate structures in the cytoplasm (Fig. 2 B). Interestingly, although NMMIIB was also localized to cell–cell junctions (Fig. S2 C), its depletion failed to alter E-cadherin localization (not depicted). Similar to NMMIIA depletion, blebbistatin treatment caused redistribution of E-cadherin immunofluorescence to the cytoplasm (Fig. 2 B). The effect of blebbistatin was rapid, altering E-cadherin localization within 24 h of treatment (Fig. 2 B).

To further dissect how NMMIIA regulates E-cadherin, we asked whether NMMIIA was necessary for E-cadherin–dependent intercellular adhesion in hESCs. We used an established adhesion assay (Verma et al., 2004) to assess the ability of cells to attach to the immobilized E-cadherin/Fc proteins (hE/Fc). In this assay, short-term blebbistatin treatment (2 h) robustly reduced the number of cells adhered to the E-cadherin substrate (Fig. 2 C), suggesting that NMMII activity is required for E-cadherin–mediated intercellular contact formation and adhesion.

NMMII-dependent cytoskeletal contractility has been implicated as a key regulator of mechanical signals in a variety of cell types including stem cells (McBeath et al., 2004; Engler et al., 2006; Chowdhury et al., 2010). In this study, we also showed that NMMII was necessary for E-cadherin–mediated mechanical tension in hESCs. We applied traction force microscopy, which assesses the mechanical interactions between cells and the substrate, to determine the traction stress in cells adhered to hE/Fc-coated substrates with an elastic modulus of 8.5 kPa. This stiffness is in the range of normal tissues (1–10 kPa), as documented previously (Janmey and McCulloch, 2007). Single H9 cells were found to exert a mean traction stress of ∼650 Pa on the substrates (Fig. 2, D and E), whereas blebbistatin treatment

(G) Quantification of the results shown in F. The y axis represents relative intensities (measured with ImageJ; National Institutes of Health) with values normalized to the signal (100%) at 0 h. Results from four separate experiments are shown. (H) Western blot analysis of E-cadherin protein in H9 cells with or without NMMIIA depletion. Asterisks indicate that the value for cells treated with blebbistatin differs statistically from the control (*, $P < 0.05$; **, $P < 0.01$; ***, $P < 0.0001$). Error bars indicate mean ± SEM.

Published October 25, 2010

markedly reduced the level of tractions (by 57%; to ∼280 Pa; Fig. 2, D and E).

Prolonged inhibition of NMMII in hESCs reduced the levels of E-cadherin protein. Blebbistatin treatment for 72 h caused both H9 and H1 cells to markedly down-regulate E-cadherin expression, which continued to decrease with longer treatments (Fig. 2, F and G; and Fig. S1 D). The reduced E-cadherin expression was also observed in MMW2 hiPSCs (Fig. S1 E), indicating conserved modulation in human pluripotent stem cells. Interestingly, down-regulation of E-cadherin was either concomitant with or preceded the down-regulation of the pluripotency proteins (Fig. 2, F and G; and Fig. S1 D). In keeping with the effect of blebbistatin, depletion of NMMIIA but not NMMIIB reduced E-cadherin levels (Fig. 2 H and not depicted). Thus, NMMIIA is required for E-cadherin–dependent intercellular adhesion and mechanical tension and modulates the levels of E-cadherin protein in hESCs.

E-cadherin serves as a bona fide target of NMMIIA in hESCs

The effect of blebbistatin and NMMIIA depletion on E-cadherin–mediated adhesion and E-cadherin expression led us to ask whether decreased E-cadherin activity and levels might be responsible for the impaired cellular compaction and stability of the OCT-4–NANOG–SOX2 circuitry.

First, we assessed the effect of DECMA-1, a function-blocking antibody that is thought to prevent homophilic binding between the E-cadherin extracellular domains (Hordijk et al., 1997). Addition of 12 µg/ml DECMA-1 (sufficient to prevent E-cadherin functions in other cells types; Hordijk et al., 1997) to H9 cell clusters failed to affect cell morphology or alter expression of pluripotency markers (unpublished data). We reasoned that the lack of inhibition might be attributed to reduced accessibility of antibodies to cells that already establish junctions, as demonstrated previously (Peignon et al., 2006). To test this, we seeded H9 cells as single cells and cultivated them in the presence of the DECMA-1 antibody, which, after a 4-d incubation with the cells, markedly reduced the number (to 36%, relative to the nonspecific IgG-treated cells) and size of cell colonies (Fig. 3, A and B; and not depicted). Furthermore, in contrast to the control cells, which grew as compact colonies with well-defined smooth edges, colonies in the presence of DECMA-1 exhibited small projections around the periphery (Fig. 3 A). Concomitant to the morphological changes, the levels of OCT-4, NANOG, SOX2, and c-Myc proteins were markedly reduced (Fig. 3 C and not depicted). Moreover, long-term treatment of cells with DECMA-1 (≥6 d) caused significant cell death (33 ± 8% vs. control cells on day 6, 5 ± 3%; $P < 0.001$), most likely because of the lack of proper intercellular adhesion.

Depletion of E-cadherin in hESCs led to similar results. Two specific shRNAs effectively depleted E-cadherin in H9 cells, produced colonies with poor cellular association, reduced the levels of OCT-4, NANOG, SOX2, and c-Myc proteins (Fig. 3, D and E; and Table S1), and induced apoptosis after prolonged depletion (E-cadherin–depleted cells, 30 ± 8%; and nontargeting shRNA control cells on day 8, 7 ± 3%; $P < 0.001$). The mRNA levels of *POU5F1*, *SOX2*, *NANOG*, and *c-Myc* were only slightly decreased (Fig. S2 D). Therefore, inhibiting E-cadherin activity or reducing E-cadherin expression in hESCs impaired cellular association, colony formation, and stability of the transcription factors. Furthermore, E-cadherin depletion mildly up-regulated markers for the three germ layers and trophoectoderm (Fig. S2 D and not depicted). The defects were highly reminiscent of those caused by NMMII inhibition or NMMIIA depletion.

Finally, overexpression of E-cadherin in hESCs nearly completely rescued the defects induced by NMMIIA depletion. Ectopic expression of E-cadherin caused H9 cells to maintain a high level of E-cadherin protein even with NMMIIA depleted. Sustained E-cadherin expression in NMMIIA-depleted cells prevented colony disruption and the down-regulation of OCT-4, NANOG, SOX2, and c-Myc (Fig. 3 F, Fig. S2 E, and not depicted). Thus, E-cadherin was capable of supporting colony formation and stability of the circuitry for pluripotency, although NMMIA expression was largely absent. Together, our results confirm and extend previous evidence (Conti et al., 2004; Shewan et al., 2005; Smutny et al., 2010), suggesting that E-cadherin serves as a bona fide target of NMMIIA in hESCs to control intercellular adhesion and the pluripotency circuitry.

NMMIIA controls E-cadherin expression via p120-catenin

p120-catenin is the prototypic member of a subfamily of Armadillo domain proteins. It binds to the juxtamembrane region of cadherin intracellular domains (Thoreson et al., 2000). p120-catenin ablation in mice and other vertebrates led to embryonic lethality (for review see McCrea and Park, 2007), demonstrating a critical role in early development. Earlier studies showed that p120-catenin regulates E-cadherin expression levels at the cell surface and modulates its signaling behavior (Davis et al., 2003; Xiao et al., 2003; Wildenberg et al., 2006). Thus, we tested the possibility that p120-catenin might be involved in the regulation of E-cadherin expression by NMMIIA.

Human cells express multiple isoforms of p120-catenin (Keirsebilck et al., 1998). Isoforms 1–4 differ from each other by the start codon used, whereas additional combinations are based on the alternative use of exons A–C. Western blot analysis of protein lysates from hESCs with two monoclonal antibodies, one against isoforms 1 and 2 (6H11; Wu et al., 1998) and the other against all isoforms (15D2; Wu et al., 1998), recognized one and two major bands, respectively (Fig. 4 A, top). A side-by-side analysis of lysates from IMR-90, a human fibroblast cell line, indicated that the band of higher molecular mass might be isoform 1 (Fig. 4 A, bottom). Mesenchymal cells such as fibroblasts express p120-catenin isoform 1 (Mo and Reynolds, 1996; Keirsebilck et al., 1998). RT-PCR analysis of alternative splicing events at the 5′ region confirmed that hESCs expressed mRNA of isoforms 1, 3, and (at a much lower level) 4 (Fig. S3 A). Based on the results from Western blot and RT-PCR analyses, we inferred that hESCs mainly express isoforms 1 and 3. In addition, RT-PCR analysis of alternative splicing at the 3′ region suggested that hESCs expressed transcripts of isoforms A and C in high abundance and, to a much lesser degree, isoform B (Fig. S3 B).

Published October 25, 2010

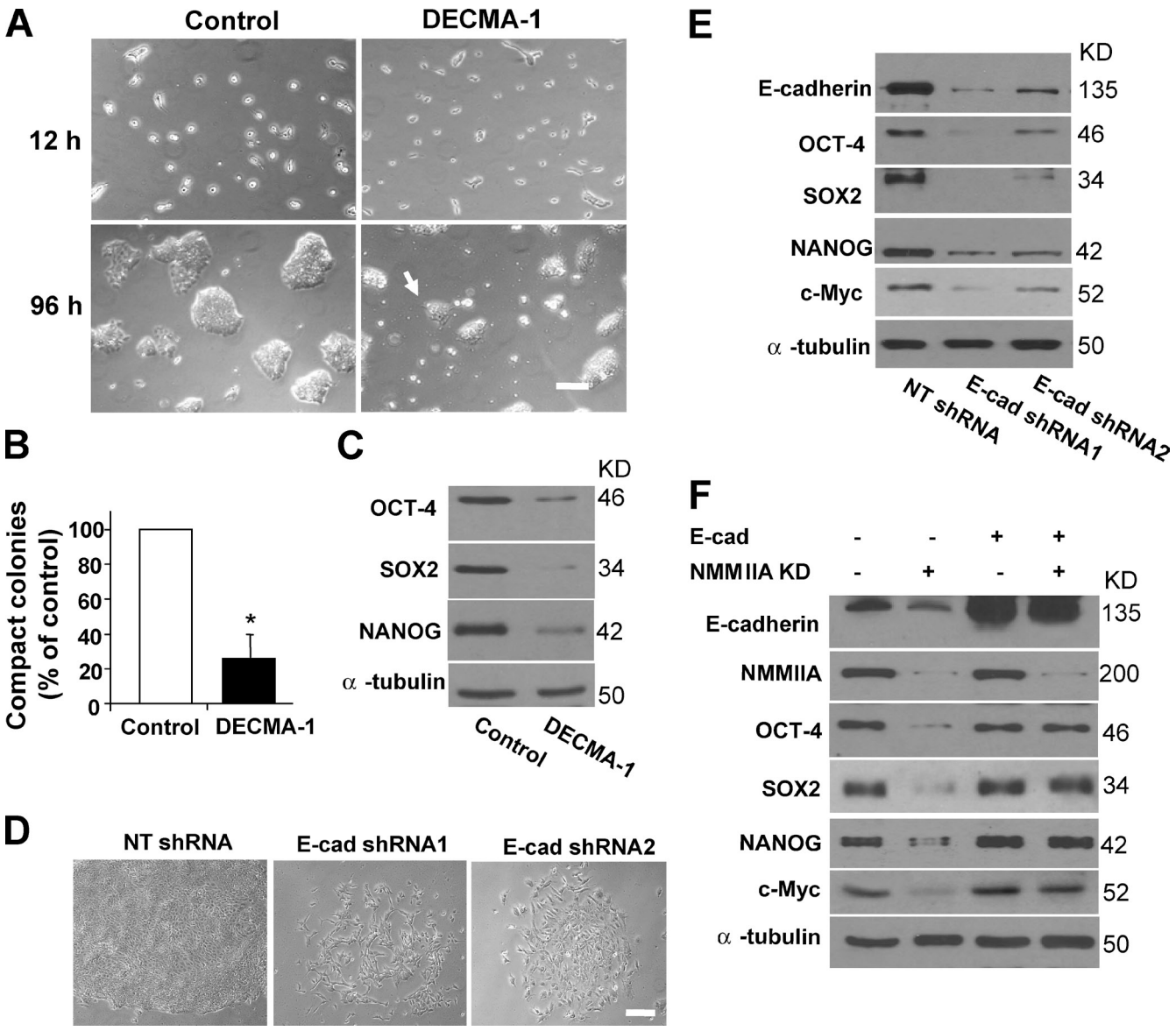

Figure 3. **E-cadherin serves as a bona fide target of NMMIIA in hESCs.** (A) Phase-contrast images of nonspecific IgG and DECMA-1–treated cells 12 and 96 h after treatments. The arrow points to an abnormal projection of a DEMCA-1–treated cell aggregate. Bar, 200 µm. (B) Quantification of colonies formed by H9 cells with IgG or DECMA-1 antibody treatment (4 d). Error bars represent the mean ± SEM of different numbers of colonies that were analyzed in multiple experiments. The values were normalized to the number (100%) of colonies formed by control cells. Asterisks indicate that the value for cells treated with DECMA-1 differs statistically from the control (*, $P < 0.05$). Cell aggregates with diameters >200 µm are defined as colonies. (C) Western blot analysis of OCT-4, NANOG, and SOX2 proteins in H9 cells treated with IgG or 12 µg/ml DECMA-1 antibody (4 d). For experiments in A–C, H9 cells were plated as single cells under feeder-free conditions and treated with nonspecific IgG or 12 µg/ml DECMA-1 antibody at the time of plating. (D) Phase-contrast images of H9 cells infected with lentivirus containing nontargeting shRNA (NT shRNA) or E-cadherin–targeting shRNAs. Bar, 100 µm. (E) Western blot analysis of E-cadherin, OCT-4, SOX2, NANOG, and c-Myc proteins in H9 cells with or without E-cadherin depletion. For experiments in D and E, cells were analyzed 4 d after infection. Qualification of the results is shown in Table S1. (F) Western blot analysis of E-cadherin, NMMIIA, OCT-4, SOX2, NANOG, and c-Myc proteins in H9 cells treated with or without E-cadherin overexpression (E-cad) and NMMIIA depletion (NMMIIA KD). Qualification of the results is shown in Fig. S2 E.

Treatment of H9 cells with blebbistatin caused marked reduction of all detectable p120-catenin protein isoforms (Fig. 4, B and C). The reduction occurred 24 h after the treatment and preceded that of E-cadherin protein (Fig. 2, F and G). Interestingly, in contrast to the reduced protein levels, the amount of p120-catenin transcripts only decreased moderately after NMMII inhibition (Fig. S3 C), indicating that the regulation occurred posttranscriptionally. In addition, short-term blebbistatin treatment (24 h) caused p120-catenin redistribution from cell–cell junctions to the cytoplasm (Fig. 4 D). In keeping with these results, NMMIIA depletion also led to substantial reduction of total p120-catenin protein (unpublished data).

In addition, p120-catenin was required for colony formation and the pluripotency maintenance circuitry of hESCs. Depletion of p120-catenin by shRNAs sharply reduced the number of hESC colonies (to 35%), induced a significant down-regulation of OCT-4, NANOG, and SOX2 (Fig. 4, E and F; and Table S1), and caused marked apoptosis after longer treatment (not depicted).

Published October 25, 2010

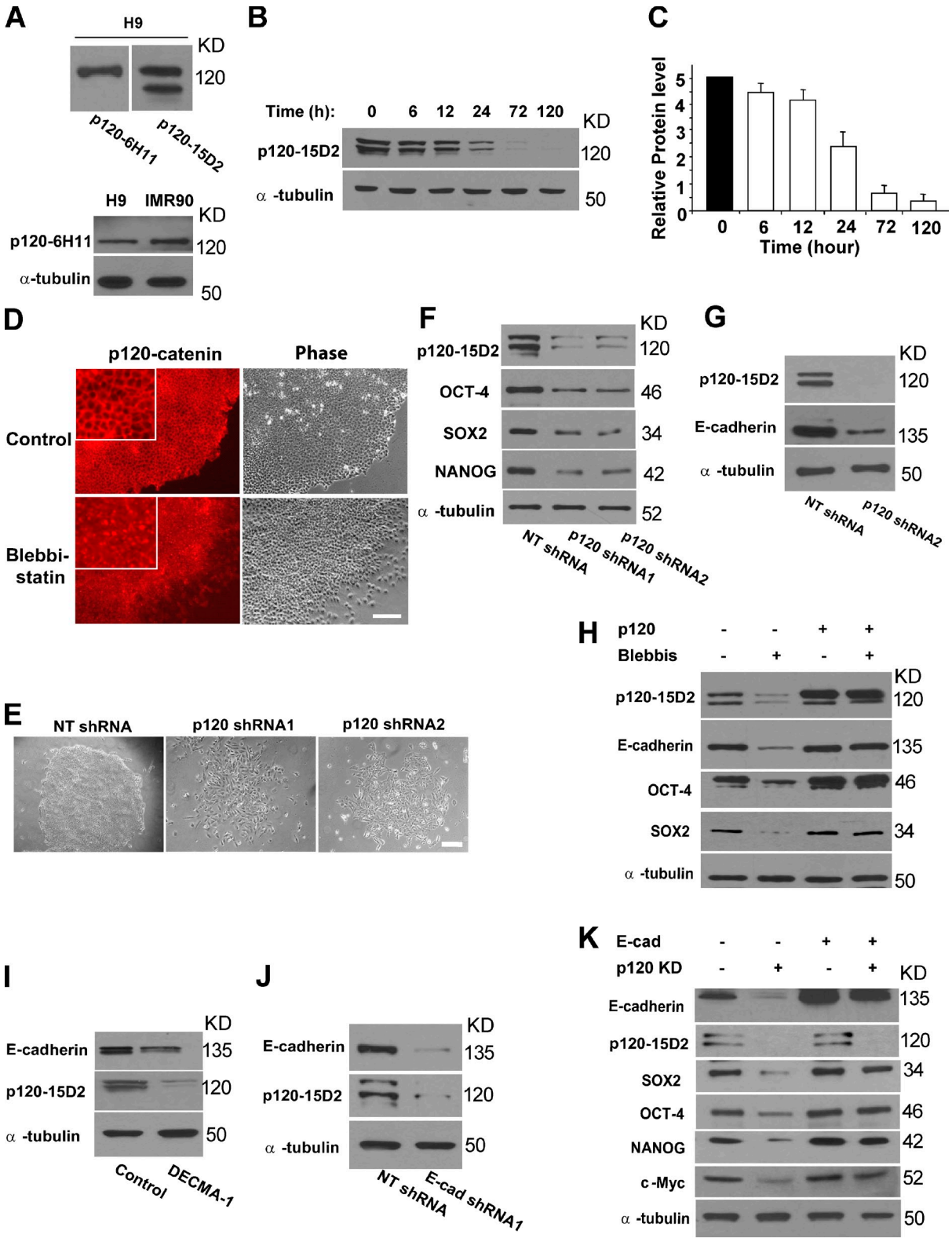

Figure 4. **NMMIIA modulates E-cadherin expression via p120-catenin.** (A) Western blot analysis of p120-catenin proteins in H9 cells. (top) Two blots showing bands recognized by 6H11 (left) or 15D2 (right) in H9 cells. (bottom) Western blot analysis of H9 and IMR-90 cell lysates with 6H11. (B) Western blot analysis of p120-catenin protein in H9 cells with or without 10 µM blebbistatin treatment for various time points. (C) Quantification of the experiment described in B. The y axis represents relative intensities (measured with ImageJ) with values normalized to the signal (100%) at 0 h. Results from four separate experiments are shown as mean ± SEM. (D) Immunofluorescence experiments of p120-catenin in H9 cells with or without blebbistatin treatment. Fluorescent images of p120-catenin staining and phase-contrast image of cells are shown. Insets show fractions of fluorescence images at a higher magnification. Cells were treated with 10 µM blebbistatin for 24 h. The monoclonal antibody 15D2 was used. (E) Phase-contrast images of H9 cells treated with nontargeting shRNA (NT shRNA) or p120-catenin–targeting shRNAs. Cells were analyzed 4 d after lentiviral infection. (D and E) Bars, 100 µm. (F) Western blot analysis of p120-catenin (with 15D2), OCT-4, NANOG, and SOX2 proteins in H9 cells with or without p120-catenin depletion for 4 d. Qualification of the results is

Published October 25, 2010

p120-catenin depletion slightly decreased *POU5F1*, *SOX2*, and *NANOG* mRNA levels and moderately up-regulated markers for the three germ layers and trophoectoderm (Fig. S3 D). These responses were highly reminiscent of those caused by E-cadherin depletion. The shRNAs used in these experiments targeted all p120 isoforms. Consistent with earlier findings (Davis et al., 2003; Xiao et al., 2003), p120-catenin depletion markedly reduced the level of E-cadherin protein in hESCs (Fig. 4 G).

Together, these data suggest that p120-catenin acts as a downstream effector of NMMIIA to regulate E-cadherin expression levels in hESCs. This inference was confirmed by the effect of ectopic expression of p120-catenin, which nearly completely rescued the decrease in E-cadherin protein levels in hESCs caused by blebbistatin treatment. In addition, p120-catenin overexpression largely rescued the defects in colony formation and the reduction in OCT-4, SOX2, and NANOG protein levels (Fig. 4 H, Fig. S3 E, and not depicted). Isoform 1A of p120-catenin, which was highly expressed in hESCs, was used for overexpression (Fig. 4 A; and Fig. S3, A and B).

p120-catenin and E-cadherin are coupled reciprocally to stabilize E-cadherin adhesion

The modulation of p120-catenin and E-cadherin appeared to be bidirectional in hESCs. Fig. 4 I shows that inhibition of E-cadherin with the DECMA-1 antibody drastically reduced the level of p120-catenin protein, which was associated with reduced E-cadherin protein levels. Similarly, depletion of E-cadherin in hESCs by shRNAs also led to reduction of p120-catenin protein levels (Fig. 4 J). Interestingly, the reciprocal modulation appears lacking in epithelial cells: the absence of E-cadherin fails to reduce the levels of p120-catenin, which becomes stranded in the cytoplasm (Thoreson et al., 2000).

It appears that the major role of p120-catenin is to support E-cadherin expression and E-cadherin–mediated intercellular adhesion, as suggested by experiments with ectopic expression of E-cadherin in hESCs with p120-catenin depletion (Fig. 4 K). We overexpressed E-cadherin in H9 cells followed by treatment with p120-catenin–targeting shRNAs. Although p120-catenin protein was nearly completely depleted, ectopic expression of E-cadherin was capable of supporting colony formation and preventing the down-regulation of OCT-4, SOX2, NANOG, and c-Myc proteins in p120-catenin–depleted cells (Fig. 4 K, Fig. S3 F, and not depicted).

Depletion of E-cadherin impairs directed somatic reprogramming

Murine and human somatic cells can be reprogrammed directly to pluripotency by ectopic expression of a subset of transcription factors (Takahashi and Yamanaka, 2006; Takahashi et al., 2007; Yu et al., 2007; Park et al., 2008). We found that E-cadherin depletion markedly reduced the efficiency of reprogramming of human primary fibroblasts and keratinocytes (Fig. S4).

The effects of depleting α- or β-catenin in hESCs

In addition to p120-catenin, the cytoplasmic domain of E-cadherin can bind directly to β-catenin, and the resulting E-cadherin–β-catenin complex binds to α-catenin. α-Catenin dynamically remodels and polymerizes the associated actin cytoskeleton at the site of cadherin-mediated cell–cell adhesion (Ozawa and Kemler, 1992; Drees et al., 2005; Yamada et al., 2005). Coupling between E-cadherin and the actin cytoskeleton is thought to be necessary for the adhesion activity of E-cadherin (Nagafuchi and Takeichi, 1988).

We asked whether α- and β-catenin play a role in the regulation of cellular association and pluripotency in hESCs. Immunofluorescence of α- and β-catenin was predominantly located at intercellular junctions of hESC colonies (Fig. 5, A and B), implying a role in the regulation of intercellular adhesion. Depletion of α- or β-catenin for 4 d mildly reduced colony formation of hESCs (to 66% and 64%, respectively) and moderately reduced the level of OCT-4, NANOG, and SOX2 proteins (Fig. 5, C–F). The effects of α- and β-catenin depletion were similar (Fig. 5 and Table S1). Notably, although >60% of the catenin-depleted colonies exhibited largely normal compact morphology, their periphery appeared to be more spread out than the control colonies (Fig. 6, C and E). These moderate defects of α- and β-catenin depletion indicate that these catenins were partially involved in the regulation of intercellular adhesion and the pluripotency circuitry in hESCs.

It was previously shown that E-cadherin homophilic binding triggers the Rac signaling pathway (Kovacs et al., 2002). Thus, we tested the possibility that Rac might mediate E-cadherin's effects on pluripotency in hESCs. Two specific shRNAs effectively depleted Rac1 in hESCs (Fig. S5 A). However, they failed to affect hESC colony formation or the expression of pluripotency markers (Fig. S5 B). These results suggest that Rac1 is not responsible for the effects of E-cadherin in hESCs.

Discussion

In conclusion, we identified critical components and signaling mechanisms that control intercellular adhesion and cellular structure, maintain stability of the transcriptional pluripotency circuitry and c-Myc expression, and support long-term survival in hESCs. A highly integrated signaling network containing NMMIIA, E-cadherin, and p120-catenin is uncovered (Fig. 6). In this network, NMMIIA regulates E-cadherin–mediated adhesion activity and the cellular levels of E-cadherin. The latter

shown in Table S1. (G) Western blot analysis of p120-catenin (15D2) and E-cadherin proteins in H9 cells 4 d after p120-catenin depletion. (H) Western blot analysis of p120-catenin (15D2), E-cadherin, OCT-4, and SOX2 proteins in H9 cells with or without isoform 1A of p120-catenin overexpression (p120) and 10 μM blebbistatin treatment for 4 d. Qualification of the results is shown in Fig. S3 E. Similar results were observed with NANOG protein (not depicted). (I) Western blot analysis of p120-catenin (15D2) and E-cadherin proteins in H9 cells 4 d after the treatment of nonspecific IgG or 12 μg/ml DECMA-1. (J) Western blot analysis of p120-catenin (15D2) and E-cadherin proteins in H9 cells 4 d after E-cadherin depletion. (K) Western blot analysis of E-cadherin, p120-catenin, OCT-4, SOX2, NANOG, and c-Myc proteins in H9 cells with or without E-cadherin overexpression and p120-catenin depletion (p120 KD) for 4 d. Qualification of the results is shown in Fig. S3 F.

Published October 25, 2010

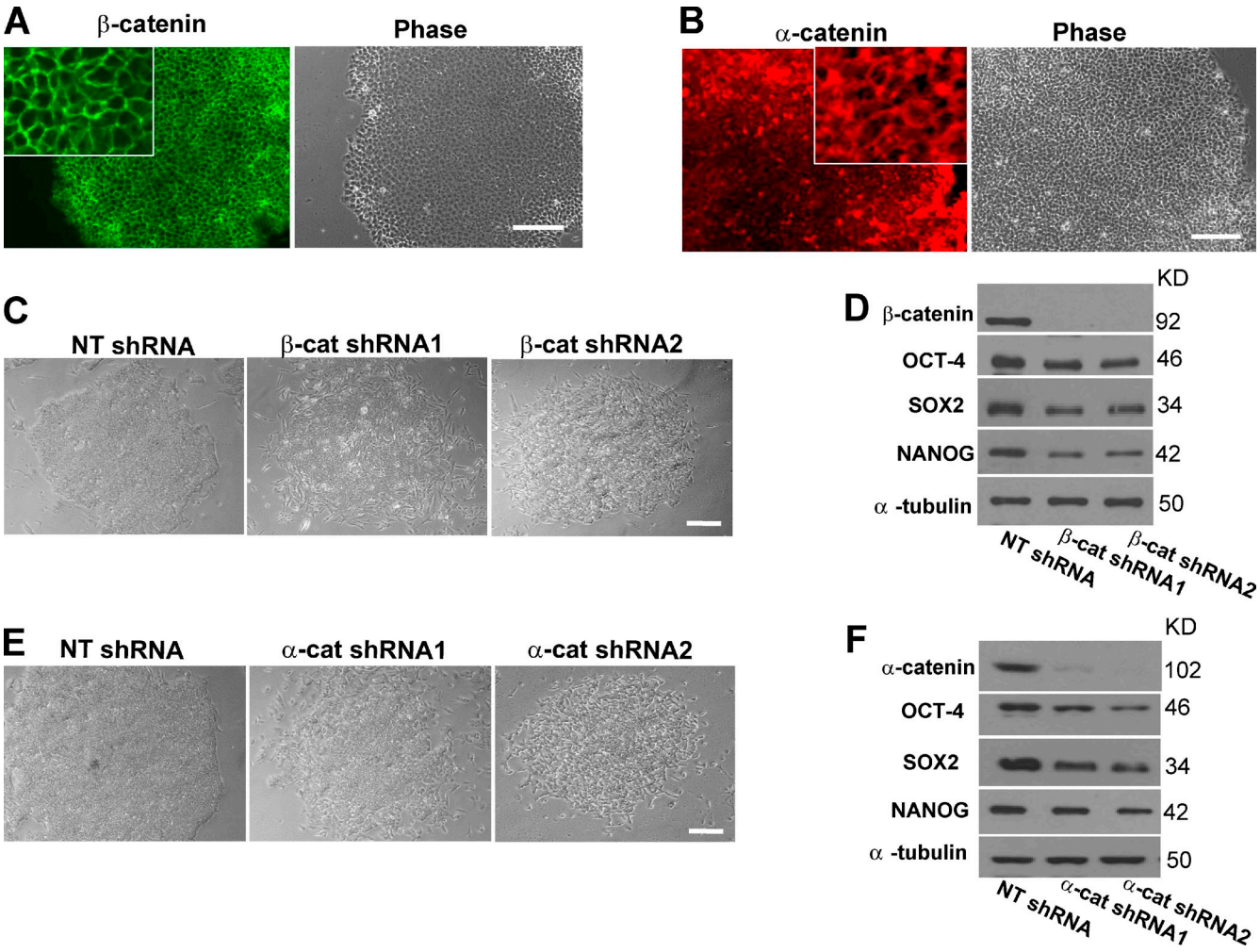

Figure 5. **The effects of depleting α- and β-catenin on colony formation and pluripotency.** (A and B) Immunofluorescence experiments of β-catenin (A) and α-catenin (B) in H9 cells. The corresponding phase-contrast images are also shown. The insets show fractions of fluorescence images at a higher magnification. (C) Phase-contrast images of H9 cells treated with nontargeting shRNA (NT shRNA) or shRNAs targeting β-catenin. (D) Western blot analysis of β-catenin, OCT-4, NANOG, and SOX2 proteins in H9 cells with or without 4-d depletion of β-catenin. (E) Phase-contrast images of H9 cells treated with nontargeting shRNA or shRNAs targeting α-catenin. (F) Western blot analysis of α-catenin, OCT-4, NANOG, and SOX2 proteins in H9 cells with or without 4-d depletion of α-catenin. (D and F) Quantification of the results is shown in Table S1. Bars, 100 µm.

response is mediated by p120-catenin, which requires NMMIIA to stabilize and in turn controls E-cadherin levels. Furthermore, we have revealed a bidirectional cross-modulation between E-cadherin and p120-catenin that promotes localized accumulation of E-cadherin at intercellular junctions. The effects of E-cadherin on hESC structures and functions might be mediated partially by α- and β-catenin or other E-cadherin–dependent mechanical and biochemical signals (Fig. 6, dashed lines). Our results unveil a mechanobiochemical mechanism central to multifaceted functions of hESCs and provide mechanistic insights into microenvironmental regulation of hESC identity.

Integration of mechanical and biochemical signals

The model in Fig. 6 suggests closely integrated mechanical and biochemical signals that cooperate to regulate intercellular adhesion and colony structures during undifferentiated growth of hESCs. In this scenario, NMMIIA-based contractility does not serve simply as a read-out of intracellular signals but, instead, plays an active role in generating or transmitting signals that control the functions of hESCs. We present evidence that NMMIIA is necessary not only for E-cadherin-mediated intercellular adhesion and mechanical tension, but also for stability of p120-catenin. Inhibition of NMMII causes the level of p120-catenin protein to decrease within 24 h, which in turn reduces E-cadherin expression levels in hESCs. Our results add to emerging evidence that cellular mechanics and myosin II-dependent cytoskeletal contractility are key regulators of fate determination in stem cells. In an earlier study, human mesenchymal stem cells (hMSCs) are shown to specify lineage and commit to phenotypes with extreme sensitivity to tissue level elasticity (Engler et al., 2006). Inhibition of NMMII blocks all elasticity directed lineage specification, implicating mechanical factors in the regulation of the directed differentiation. In a separate study, McBeath et al. (2004) showed that cell shape regulates commitment of hMSCs to adipocyte or osteoblast fate, which requires actin-myosin-generated tension. The critical role of mechanical and physical factors has also been revealed in pluripotent

Published October 25, 2010

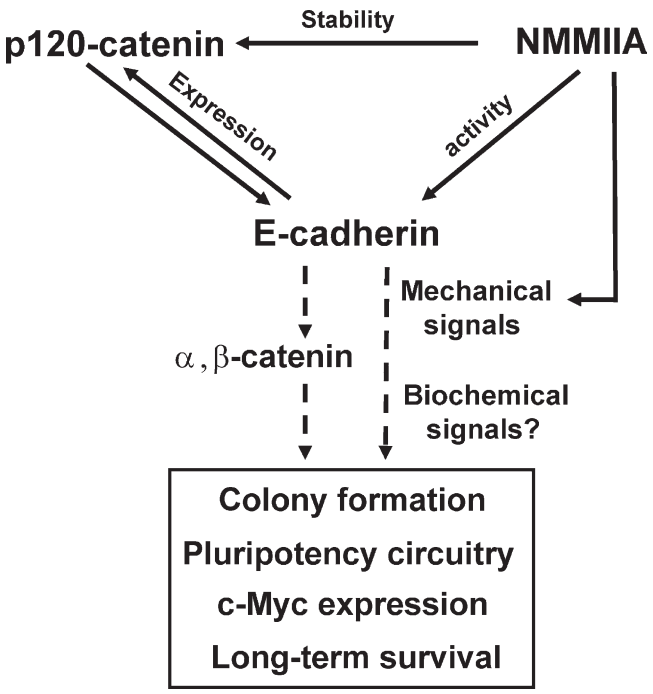

Figure 6. **Integrated biochemical and mechanical signals regulate multifaceted functions of hESCs.** A model is shown. See Discussion for details.

stem cells. Application of local stress induces cell spreading and down-regulation of OCT-4 in mESCs, and the spreading and down-regulation depend upon NMMII activity (Chowdhury et al., 2010). Our results provide an additional example of mechanical regulation of fate decisions in stem cells. In addition, our data begin to reveal some molecular details underlying the integration of mechanical and biochemical signals.

Our findings suggest a potential positive feedback loop that controls localized accumulation of E-cadherin at the intercellular adhesion sites of hESCs. The components of the feedback loop include E-cadherin and p120-catenin. First, inhibition (or depletion) of one protein markedly decreases the level of the other, demonstrating bidirectional regulation between them. Furthermore, phenotypes of hESCs with E-cadherin or p120-catenin depletion are remarkably similar. One arc of the feedback loop, in which p120-catenin regulates the cellular levels of E-cadherin, is in keeping with the previously reported role of p120-catenin in stabilizing cadherin junctions in cell types including epithelial and endothelial cells (Davis et al., 2003; Xiao et al., 2003). Interestingly, the reciprocal arc, in which E-cadherin modulates the accumulation of p120-catenin, has not been documented. In epithelial cells, the absence of E-cadherin fails to reduce the levels of p120-catenin, which instead becomes stranded in the cytoplasm (Thoreson et al., 2000). Thus, the potential feedback loop might be a feature uniquely related to the identity of ESCs. We envision that the positive feedback regulation could lead to rapid and robust accumulation of E-cadherin protein at the intercellular junctions, thus allowing hESCs to quickly establish, consolidate, and strengthen their cellular association and colony structures during undifferentiated growth. Interestingly, the stability of the putative feedback loop depends on the input from NMMIIA, which controls E-cadherin levels via p120-catenin. We also envision that integration of mechanical regulation with the biochemical signals may provide greater robustness to the feedback loop and create additional levels of regulation for E-cadherin–mediated intercellular adhesion, which might be essential for the diverse fate decisions hESCs (or other pluripotent stem cells) are poised to make in response to various extrinsic an intrinsic cues. More complete understanding of the detailed mechanisms underlying the feedback regulation and mechanical–biochemical integration awaits future experimentation.

How might E-cadherin regulate the transcriptional circuitry for pluripotency?

Our data confirm and extend previous evidence, suggesting that the OCT-4–SOX2–NANOG circuitry is intimately linked to intercellular adhesion and colony integrity of hESCs during undifferentiated growth. Disruption of cellular association and compact structures of hESCs in each case causes concomitant down-regulation of the transcription factors. Our results have also assigned an essential role for E-cadherin in the maintenance of the hESC circuitry: depletion or inhibition of E-cadherin induces down-regulation of OCT-4, SOX2, and NANOG within 4 d. Although inhibition (or depletion) of NMMIIA and p120-catenin leads to similar defects, our findings suggest that the effects of NMMIIA and p120-catenin are mediated by E-cadherin. Ectopic expression of E-cadherin in hESCs supports stability of the pluripotency circuitry, although NMMIIA and p120 catenin are largely absent.

How might E-cadherin–mediated cell–cell adhesion regulate the transcriptional circuitry for pluripotency? Our results imply two possible mechanisms. First, α- or β-catenin depletion produces defects that partially recapitulate those caused by E-cadherin depletion/inhibition. Recent studies demonstrated that cadherin clusters at the plasma membranes cause the release of α-catenin dimers, which in turn induces actin bundling by reportedly competing with Arp2/3-binding sites on actin (Drees et al., 2005; Yamada et al., 2005). Thus, these results indicate that dynamic actin assembly mediated by the interactions between E-cadherin and α- and β-catenin might be partially involved in the signal transduction from intercellular adhesion sites to the nuclear pluripotency circuitry (Fig. 6). Second, we show that E-cadherin–mediated adhesion induces mechanical tension, which could transduce information to influence the pluripotency network (Fig. 6, dashed lines). Other speculative mechanisms alone or in combination could also contribute to the cross-modulation between cellular compaction and pluripotency. Unidentified molecular components downstream of E-cadherin adhesion in hESCs could transmit signals to stabilize the core transcriptional circuitry. In addition, it might be that E-cadherin–dependent intercellular adhesion is a prerequisite for the activation of pluripotency-promoting signaling pathways such as those mediated by bFGF, TGF-β, and mTOR.

Materials and methods

Cell culture

hESC lines H9 and H1 (WiCell Research Institute, Madison, WI) were routinely maintained under feeder conditions as previously described (Thomson et al., 1998). In brief, primary mouse embryonic fibroblasts (MEFs) prepared

Published October 25, 2010

from embryos of pregnant CF-1 mice (day 13.5 of gestation; Charles River) were cultured in Dulbecco's minimum essential medium (DMEM) containing 10% FBS (Hyclone) and 1 mM nonessential amino acid and penicillin/streptomycin and mitotically inactivated by γ-irradiation. H1 and H9 cells were cultured on irradiated MEFs in media containing DMEM/F12, 20% knockout serum replacement, 4 ng/ml bFGF (Invitrogen), 1% nonessential amino acid, 1 mM glutamine, and 0.1 mM β-mercaptoethanol. For feeder-free cultures, cells were cultured on Matrigel (BD)-coated plates in MEF-conditioned medium as previously described (Xu et al., 2001). MMW2 hiPSCs (Mali et al., 2010) were cultured under the same conditions as hESCs. W4/129 mESCs (Taconic) were cultured on 0.1% gelatin-coated 6-well plates in media containing DMEM (high glucose; Invitrogen), 15% FBS, 1,000 U/ml LIF (Millipore), 0.1 mM nonessential amino acids, 2 mM L-glutamine, 1 mM sodium pyruvate, 10^{-6} M 2-mercaptoethanol, and 100 U/ml penicillin/streptomycin. Medium changes were administered every other day. HEK293T, HT29, and IMR90 cells were purchased from American Type Culture Collection (ATCC) and cultured following ATCC recommendations.

Inhibitor and antibodies

Blebbistatin was purchased from EMD. Rat monoclonal antibody against E-cadherin (DECMA-1) was obtained from Abcam. Antibodies against p120-catenin (15D2 and 6H11) were described previously (Wu et al., 1998). The polyclonal antibody against α-catenin was provided by B. Gumbiner (University of Virginia, Charlottesville, VA; Funayama et al., 1995). Alexa Fluor 488– and 594–conjugated secondary antibodies were obtained from Invitrogen. All antibodies for Western and/or immunofluorescence analyses are listed in Table S2.

DNA constructs

Full-length E-cadherin cDNA was amplified from pCDNA3 containing human E-cadherin–YFP (provided by A. Yap, The University of Queensland, Brisbane, Queensland, Australia) by PCR using forward primer hE-cad-wt-F (Table S4) and reverse primer hE-cad-wt-R (Table S4). The PCR product was cloned into PCR8/GW/TOPO entry vector (Invitrogen). The final overexpression construct was attained by recombination of the resulting entry clone with the pENTR TOPO vector containing the EF1-α promoter and the 2k7neo lentiviral vector as previously described (Zhou et al., 2009). Positive clones containing the EF-1-α promoter and human E-cadherin cDNA were confirmed by sequencing.

Full-length human p120 1A cDNA was amplified from pMS containing isoform 1A of human p120-catenin by PCR using forward primer hp120-1AF (Table S4) and reverse primer hp120-1AR (Table S4) modified to contain SpeI and EcoRI recognition sites, respectively. The PCR product was ligated into pSin-EF2-Nanog-Pur (Addgene) by replacing NANOG cDNA after SpeI and EcoRI restriction digestions. Positive clones were verified by sequencing.

Lentivirus production and hESC infection

For shRNA-mediated gene knockdown, pLKO vectors containing different shRNA sequences (Sigma-Aldrich; Table S3) were used to package virus with Viralpower Lentivirus Packaging System (Invitrogen) as previously described (Zhou et al., 2009). For lentiviral infection, hESCs cultured on MEFs were dissociated as clusters and plated onto Matrigel-coated plates. Lentivirus (MOI, 10–200) was directly added into MEF-conditioned medium containing 6 µg/ml polybrene (Sigma-Aldrich) and incubated for ∼20 h before medium change. Selection commenced 48 h after infection with 2 ug/ml puromycin. Cells were analyzed 4–5 d after selection.

For ectopic expression of human E-cadherin and p120-catenin in hESCs, lentiviral-mediated delivery and selection (400 µg/ml G418 or 2 µg/ml puromycin, respectively) were performed after the aforementioned procedures. For combined overexpression and depletion experiments, cells were coinfected with shRNA and overexpression cassette lentivirus followed by selection and analysis.

Induction of directed reprogramming

The lentiviral constructs containing overexpression cassettes for OCT-4, SOX2, NANOG, Lin-28, KLF4, and c-Myc were obtained from Addgene. Lentivirus for the six factors was mixed at equal amounts in media containing 6 µg/ml polybrene and administered to IMR-90 (passages 1–5; ATCC) or human neonatal keratinocytes (passages 1–5; Invitrogen) together with lentivirus containing nontargeting shRNA or E-cadherin–targeting shRNA. 48 h after infection, cells (10^7 cells) were dissociated into single cells by trypsin and plated onto culture dishes coated with γ-irradiated MEFs. Cell colonies typically emerged within 4–6 (keratinocytes) or 8–9 d (IMR-90). The number of ESC-like colonies was counted 2 wk after the initial plating. ESC-like colonies were scored based on morphology and AP activity. Reprogramming efficiency was calculated as the number of ESC-like colonies divided by the total number of cells plated on MEFs after infection.

Western blotting

Cells were lysed directly with Laemmli 2× sample buffer (Bio-Rad Laboratories). Lysates were separated by SDS-PAGE and analyzed by Western blotting. Dilutions used for various antibodies are described in Table S2. The blots were developed using SuperSignal West Pico Chemiluminescent Substrate (Thermo Fisher Scientific).

Immunofluorescence

hESCs cultured under feeder-free conditions were washed twice with cold PBS, fixed with 3.7% paraformaldehyde for 20 min at room temperature, permeabilized with 0.1% Triton X-100 in PBS, and blocked with PBS containing 2% normal donkey serum. Samples were incubated overnight at 4°C with primary antibody (Table S2) followed by two washes with PBS and a 1-h room temperature incubation with Alexa Fluor 488 (or 594)–conjugated secondary antibody. Nuclei were counterstained with DAPI (Sigma-Aldrich) for 5 min. Phase-contrast and fluorescent images were collected with a 10× 0.3 NA EC Plan Neofluar Ph1 objective (Carl Zeiss, Inc.) on a microscope (Axiovert 200M; Carl Zeiss, Inc.). All images were collected with a cooled charge-coupled device camera (AxioCam MR3; Carl Zeiss, Inc.) at room temperature and processed using Photoshop (Adobe).

AP staining

An AP detection kit (Millipore) was used following the manufacturer's instructions. In brief, cells were fixed with 4% paraformaldehyde for 2 min and washed and stained with the staining solution for 15 min at room temperature. After three washes, cells were visualized using light microscopy.

RNA preparation and real-time PCR

For real-time PCR, total RNA was isolated from cells with Trizol reagent (Invitrogen) and purified with RNeasy mini kit (QIAGEN) following the manufacturer's instructions. cDNA was synthesized from the purified RNA using a reverse transcription system (Promega) with random primers. Real-time PCR was performed using SYBR green PCR kit (QuantiTech; QIAGEN). Reactions were performed in 25 µl containing 2× 12.5 µl SYBR green mix, 10× primer solution (2.5 µl mixture of forward and reverse primers), 2 µl cDNA, and nuclease-free water. The PCR program following QIAGEN protocols was used as described previously (Zhou et al., 2009): 95°C for 15 min followed by 40 cycles of 94°C for 15 s, 56°C for 15 s, and 72°C for 34 s. All gene-specific primers were generated based on sequences at PrimerBank or purchased from QIAGEN (Table S4). β-Actin was used to normalize gene expression levels.

RT-PCR analysis of p120-catenin isoforms

The pattern of p120-catenin expression in hESCs was analyzed as described previously (Keirsebilck et al., 1998). In brief, total RNA was prepared from hESCs, and cDNA was synthesized from the purified RNA using a reverse transcription system (Promega) with oligo(dT) primers. The synthesized cDNA was amplified by PCR in reactions containing cDNA template, p120-catenin isoform-specific primers (Table S4), 0.25 U Taq DNA polymerase, and deoxynucleoside 5′-triphosphates. The following program was used: 94°C for 5 min, 80°C for 1 min followed by 35 cycles of 94°C for 1 min, 55°C for 45 s, 72°C for 1.5 min, and a final extension at 72°C for 10 min. The PCR products were analyzed on a 1.5% agarose gel.

E-cadherin adhesion assay

Adhesion of hESCs to hE/Fc-coated substrata was measured by the resistance to detachment as previously described (Verma et al., 2004). In brief, nitrocellulose-coated 96-well plates were incubated with 0.1% hE/Fc (in HBSS containing 5 mM $CaCl_2$) overnight at 4°C. The plate was blocked with 10 mg/ml bovine serum albumin for 2 h at 4°C. H9 cells were pretreated with Y-27632 for 2 h and digested with accutase (Invitrogen) for 7 min. Freshly isolated cells were allowed to attach to substrata for 2 h at 37°C in a CO_2 incubator with or without 10 µM blebbistatin and subjected to detachment by shear stress created by systematic pipetting. Cells remaining adherent to the wells were incubated with calcain-AM for 30 min, washed, and measured with a fluorescence plate reader (λEX, 485 nm; and λEM, 535 nm; CytoFluor 2300; Millipore).

Apoptosis assay

To determine the rate of apoptosis in hESCs, H9 cells with or without various treatments were dissociated into single cells using 0.25% trysin-EDTA

(Invitrogen) at 37°C for 10 min. Apoptosis was measured using the annexin-V–FITC Apoptosis Detection kit (BD). In brief, cells were washed with cold PBS then resuspended in binding buffer. 5 µl annexin-V–FITC and 5 µl propidium iodide were added to the suspension and incubated for 20 min at room temperature. Cells were subsequently analyzed using FACSDiva (BD). Cells that detected as annexin-V positive and propidium iodide negative were counted as apoptotic cells.

Polyacrylamide gel substrates, traction force microscopy, and data analysis

Polyacrylamide gels were prepared as described previously (Pelham and Wang, 1999). 0.2 µm red fluorescent microspheres (Invitrogen) were embedded in 75-µm-thick gels for traction detection, and the gels were coated with 0.1% hE/Fc. The elastic Young modulus of the polyacrylamide gels was 8.5 kPa (5% acrylamide and 0.3% *bis*-acrylamide; Engler et al., 2004). Experiments and analysis were performed as described previously (Butler et al., 2002; Tolić-Nørrelykke et al., 2002). In brief, hESCs pretreated with or without 10 µM blebbistatin for 1 h were plated as single cells and allowed to adhere to the hE/Fc-coated polyacrylamide gel for 1 h at 37°C. Cells were initially round upon binding to E-cadherin then spread onto the substrate 1 h after plating. 10 µM blebbistatin was also included during the period of cell plating. Traction force microscopy was performed using a microscope (Axiovert 200M) with a 40× 1.30 NA Fluar differential interference contrast objective lens. Images of cells and fluorescent beads were captured interchangeably every 10 s for 10 times using a cooled charge-coupled device camera (AxioCam MR3; Carl Zeiss, Inc.). Images of the beads were analyzed by a custom-made program to calculate bead displacement and generate traction maps. Images of beads after cell detachment, representing the traction-free state, were used as a reference.

Online supplemental material

Fig. S1 shows the effects of blebbistatin in hESCs and other pluripotent stem cells. Fig. S2 shows additional results from E-cadherin depletion and overexpression. Fig. S3 shows additional results for p120-catenin expression profile, depletion, and overexpression. Fig. S4 shows that E-cadherin depletion impairs directed reprogramming of human somatic cells. Fig. S5 shows Rac1 depletion in hESCs. Table S1 shows expression of pluripotency proteins and colony formation in hESCs with various treatments. Table S2 shows sources and dilutions of antibodies. Table S3 shows shRNA sequences and their targets. Table S4 shows the names and sequences of primers used in this study. Online supplemental material is available at http://www.jcb.org/cgi/content/full/jcb.201006094/DC1.

We thank Dr. Barry Gumbiner for providing the α-catenin antibodies, Dr. Alpha Yap for providing the human E-cadherin–YFP construct, Dr. Elvira de Mejia for providing HT29 cells, and Dr. William Brieher and members of the Wang laboratory for helpful discussions.

This work was supported by grants from National Institutes of Health (GM-83812 to F. Wang) and the Illinois Regenerative Medicine Institute (IDPH 2006-05516 to F. Wang and T.S. Tanaka) and by the National Science Foundation CAREER award (0953267 to F. Wang) and the Beckman award from the University of Illinois and the National Natural Science Foundation of China (30728022 to F. Wang and E. Duan). Research conducted in the Cheng laboratory at Johns Hopkins University is supported in part by the National Institutes of Health (grants RC2 HL101582 and U01 HL099775).

Submitted: 18 June 2010
Accepted: 28 September 2010

References

Bendall, S.C., M.H. Stewart, P. Menendez, D. George, K. Vijayaragavan, T. Werbowetski-Ogilvie, V. Ramos-Mejia, A. Rouleau, J. Yang, M. Bossé, et al. 2007. IGF and FGF cooperatively establish the regulatory stem cell niche of pluripotent human cells in vitro. *Nature.* 448:1015–1021. doi:10.1038/nature06027

Butler, J.P., I.M. Tolić-Nørrelykke, B. Fabry, and J.J. Fredberg. 2002. Traction fields, moments, and strain energy that cells exert on their surroundings. *Am. J. Physiol. Cell Physiol.* 282:C595–C605.

Chowdhury, F., S. Na, D. Li, Y.C. Poh, T.S. Tanaka, F. Wang, and N. Wang. 2010. Material properties of the cell dictate stress-induced spreading and differentiation in embryonic stem cells. *Nat. Mater.* 9:82–88. doi:10.1038/nmat2563

Constantinescu, D., H.L. Gray, P.J. Sammak, G.P. Schatten, and A.B. Csoka. 2006. Lamin A/C expression is a marker of mouse and human embryonic stem cell differentiation. *Stem Cells.* 24:177–185. doi:10.1634/stemcells.2004-0159

Conti, M.A., S. Even-Ram, C. Liu, K.M. Yamada, and R.S. Adelstein. 2004. Defects in cell adhesion and the visceral endoderm following ablation of nonmuscle myosin heavy chain II-A in mice. *J. Biol. Chem.* 279:41263–41266. doi:10.1074/jbc.C400352200

Cowin, P., and B. Burke. 1996. Cytoskeleton-membrane interactions. *Curr. Opin. Cell Biol.* 8:56–65. doi:10.1016/S0955-0674(96)80049-4

Daley, G.Q., and D.T. Scadden. 2008. Prospects for stem cell-based therapy. *Cell.* 132:544–548. doi:10.1016/j.cell.2008.02.009

Davis, M.A., R.C. Ireton, and A.B. Reynolds. 2003. A core function for p120-catenin in cadherin turnover. *J. Cell Biol.* 163:525–534. doi:10.1083/jcb.200307111

Drees, F., S. Pokutta, S. Yamada, W.J. Nelson, and W.I. Weis. 2005. Alpha-catenin is a molecular switch that binds E-cadherin-beta-catenin and regulates actin-filament assembly. *Cell.* 123:903–915. doi:10.1016/j.cell.2005.09.021

Engler, A., L. Bacakova, C. Newman, A. Hategan, M. Griffin, and D. Discher. 2004. Substrate compliance versus ligand density in cell on gel responses. *Biophys. J.* 86:617–628. doi:10.1016/S0006-3495(04)74140-5

Engler, A.J., S. Sen, H.L. Sweeney, and D.E. Discher. 2006. Matrix elasticity directs stem cell lineage specification. *Cell.* 126:677–689. doi:10.1016/j.cell.2006.06.044

Fang, X., H. Ji, S.W. Kim, J.I. Park, T.G. Vaught, P.Z. Anastasiadis, M. Ciesiolka, and P.D. McCrea. 2004. Vertebrate development requires ARVCF and p120 catenins and their interplay with RhoA and Rac. *J. Cell Biol.* 165:87–98. doi:10.1083/jcb.200307109

Funayama, N., F. Fagotto, P. McCrea, and B.M. Gumbiner. 1995. Embryonic axis induction by the armadillo repeat domain of β-catenin: evidence for intracellular signaling. *J. Cell Biol.* 128:959–968. doi:10.1083/jcb.128.5.959

Gumbiner, B.M. 2005. Regulation of cadherin-mediated adhesion in morphogenesis. *Nat. Rev. Mol. Cell Biol.* 6:622–634. doi:10.1038/nrm1699

Haegel, H., L. Larue, M. Ohsugi, L. Fedorov, K. Herrenknecht, and R. Kemler. 1995. Lack of beta-catenin affects mouse development at gastrulation. *Development.* 121:3529–3537.

Hordijk, P.L., J.P. ten Klooster, R.A. van der Kammen, F. Michiels, L.C. Oomen, and J.G. Collard. 1997. Inhibition of invasion of epithelial cells by Tiam1-Rac signaling. *Science.* 278:1464–1466. doi:10.1126/science.278.5342.1464

Jaenisch, R., and R. Young. 2008. Stem cells, the molecular circuitry of pluripotency and nuclear reprogramming. *Cell.* 132:567–582. doi:10.1016/j.cell.2008.01.015

Janmey, P.A., and C.A. McCulloch. 2007. Cell mechanics: integrating cell responses to mechanical stimuli. *Annu. Rev. Biomed. Eng.* 9:1–34. doi:10.1146/annurev.bioeng.9.060906.151927

Keirsebilck, A., S. Bonné, K. Staes, J. van Hengel, F. Nollet, A. Reynolds, and F. van Roy. 1998. Molecular cloning of the human p120ctn catenin gene (CTNND1): expression of multiple alternatively spliced isoforms. *Genomics.* 50:129–146. doi:10.1006/geno.1998.5325

Kovacs, E.M., R.G. Ali, A.J. McCormack, and A.S. Yap. 2002. E-cadherin homophilic ligation directly signals through Rac and phosphatidylinositol 3-kinase to regulate adhesive contacts. *J. Biol. Chem.* 277:6708–6718. doi:10.1074/jbc.M109640200

Levenstein, M.E., T.E. Ludwig, R.H. Xu, R.A. Llanas, K. VanDenHeuvel-Kramer, D. Manning, and J.A. Thomson. 2006. Basic fibroblast growth factor support of human embryonic stem cell self-renewal. *Stem Cells.* 24:568–574. doi:10.1634/stemcells.2005-0247

Li, L., S. Wang, A. Jezierski, L. Moalim-Nour, K. Mohib, R.J. Parks, S.F. Retta, and L. Wang. 2010. A unique interplay between Rap1 and E-cadherin in the endocytic pathway regulates self-renewal of human embryonic stem cells. *Stem Cells.* 28:247–257.

Mali, P., B.K. Chou, J. Yen, Z. Ye, J. Zou, S. Dowey, R.A. Brodsky, J.E. Ohm, W. Yu, S.B. Baylin, et al. 2010. Butyrate greatly enhances derivation of human induced pluripotent stem cells by promoting epigenetic remodeling and the expression of pluripotency-associated genes. *Stem Cells.* 28:713–720. doi:10.1002/stem.402

McBeath, R., D.M. Pirone, C.M. Nelson, K. Bhadriraju, and C.S. Chen. 2004. Cell shape, cytoskeletal tension, and RhoA regulate stem cell lineage commitment. *Dev. Cell.* 6:483–495. doi:10.1016/S1534-5807(04)00075-9

McCrea, P.D., and J.I. Park. 2007. Developmental functions of the P120-catenin sub-family. *Biochim. Biophys. Acta.* 1773:17–33. doi:10.1016/j.bbamcr.2006.06.009

Mo, Y.Y., and A.B. Reynolds. 1996. Identification of murine p120 isoforms and heterogeneous expression of p120cas isoforms in human tumor cell lines. *Cancer Res.* 56:2633–2640.

Nagafuchi, A., and M. Takeichi. 1988. Cell binding function of E-cadherin is regulated by the cytoplasmic domain. *EMBO J.* 7:3679–3684.

Published October 25, 2010

Okita, K., and S. Yamanaka. 2006. Intracellular signaling pathways regulating pluripotency of embryonic stem cells. *Curr. Stem Cell Res. Ther.* 1:103–111. doi:10.2174/157488806775269061

Ozawa, M., and R. Kemler. 1992. Molecular organization of the uvomorulin-catenin complex. *J. Cell Biol.* 116:989–996. doi:10.1083/jcb.116.4.989

Park, I.H., R. Zhao, J.A. West, A. Yabuuchi, H. Huo, T.A. Ince, P.H. Lerou, M.W. Lensch, and G.Q. Daley. 2008. Reprogramming of human somatic cells to pluripotency with defined factors. *Nature.* 451:141–146. doi:10.1038/nature06534

Peignon, G., S. Thenet, C. Schreider, S. Fouquet, A. Ribeiro, E. Dussaulx, J. Chambaz, P. Cardot, M. Pinçon-Raymond, and J. Le Beyec. 2006. E-cadherin-dependent transcriptional control of apolipoprotein A-IV gene expression in intestinal epithelial cells: a role for the hepatic nuclear factor 4. *J. Biol. Chem.* 281:3560–3568. doi:10.1074/jbc.M506360200

Pelham, R.J. Jr., and Y. Wang. 1999. High resolution detection of mechanical forces exerted by locomoting fibroblasts on the substrate. *Mol. Biol. Cell.* 10:935–945.

Rossant, J. 2008. Stem cells and early lineage development. *Cell.* 132:527–531. doi:10.1016/j.cell.2008.01.039

Shewan, A.M., M. Maddugoda, A. Kraemer, S.J. Stehbens, S. Verma, E.M. Kovacs, and A.S. Yap. 2005. Myosin 2 is a key Rho kinase target necessary for the local concentration of E-cadherin at cell-cell contacts. *Mol. Biol. Cell.* 16:4531–4542. doi:10.1091/mbc.E05-04-0330

Smutny, M., H.L. Cox, J.M. Leerberg, E.M. Kovacs, M.A. Conti, C. Ferguson, N.A. Hamilton, R.G. Parton, R.S. Adelstein, and A.S. Yap. 2010. Myosin II isoforms identify distinct functional modules that support integrity of the epithelial zonula adherens. *Nat. Cell Biol.* 12:696–702. doi:10.1038/ncb2072

Straight, A.F., A. Cheung, J. Limouze, I. Chen, N.J. Westwood, J.R. Sellers, and T.J. Mitchison. 2003. Dissecting temporal and spatial control of cytokinesis with a myosin II Inhibitor. *Science.* 299:1743–1747. doi:10.1126/science.1081412

Takahashi, K., and S. Yamanaka. 2006. Induction of pluripotent stem cells from mouse embryonic and adult fibroblast cultures by defined factors. *Cell.* 126:663–676. doi:10.1016/j.cell.2006.07.024

Takahashi, K., K. Tanabe, M. Ohnuki, M. Narita, T. Ichisaka, K. Tomoda, and S. Yamanaka. 2007. Induction of pluripotent stem cells from adult human fibroblasts by defined factors. *Cell.* 131:861–872. doi:10.1016/j.cell.2007.11.019

Takeichi, M. 1995. Morphogenetic roles of classic cadherins. *Curr. Opin. Cell Biol.* 7:619–627. doi:10.1016/0955-0674(95)80102-2

Thomson, J.A., J. Itskovitz-Eldor, S.S. Shapiro, M.A. Waknitz, J.J. Swiergiel, V.S. Marshall, and J.M. Jones. 1998. Embryonic stem cell lines derived from human blastocysts. *Science.* 282:1145–1147. doi:10.1126/science.282.5391.1145

Thoreson, M.A., P.Z. Anastasiadis, J.M. Daniel, R.C. Ireton, M.J. Wheelock, K.R. Johnson, D.K. Hummingbird, and A.B. Reynolds. 2000. Selective uncoupling of p120(^{ctn}) from E-cadherin disrupts strong adhesion. *J. Cell Biol.* 148:189–202. doi:10.1083/jcb.148.1.189

Tolić-Nørrelykke, I.M., J.P. Butler, J. Chen, and N. Wang. 2002. Spatial and temporal traction response in human airway smooth muscle cells. *Am. J. Physiol. Cell Physiol.* 283:C1254–C1266.

Torres, M., A. Stoykova, O. Huber, K. Chowdhury, P. Bonaldo, A. Mansouri, S. Butz, R. Kemler, and P. Gruss. 1997. An alpha-E-catenin gene trap mutation defines its function in preimplantation development. *Proc. Natl. Acad. Sci. USA.* 94:901–906. doi:10.1073/pnas.94.3.901

Tullio, A.N., D. Accili, V.J. Ferrans, Z.X. Yu, K. Takeda, A. Grinberg, H. Westphal, Y.A. Preston, and R.S. Adelstein. 1997. Nonmuscle myosin II-B is required for normal development of the mouse heart. *Proc. Natl. Acad. Sci. USA.* 94:12407–12412. doi:10.1073/pnas.94.23.12407

Verma, S., A.M. Shewan, J.A. Scott, F.M. Helwani, N.R. den Elzen, H. Miki, T. Takenawa, and A.S. Yap. 2004. Arp2/3 activity is necessary for efficient formation of E-cadherin adhesive contacts. *J. Biol. Chem.* 279:34062–34070. doi:10.1074/jbc.M404814200

Wang, L., T.C. Schulz, E.S. Sherrer, D.S. Dauphin, S. Shin, A.M. Nelson, C.B. Ware, M. Zhan, C.Z. Song, X. Chen, et al. 2007. Self-renewal of human embryonic stem cells requires insulin-like growth factor-1 receptor and ERBB2 receptor signaling. *Blood.* 110:4111–4119. doi:10.1182/blood-2007-03-082586

Watanabe, K., M. Ueno, D. Kamiya, A. Nishiyama, M. Matsumura, T. Wataya, J.B. Takahashi, S. Nishikawa, S. Nishikawa, K. Muguruma, and Y. Sasai. 2007. A ROCK inhibitor permits survival of dissociated human embryonic stem cells. *Nat. Biotechnol.* 25:681–686. doi:10.1038/nbt1310

Wildenberg, G.A., M.R. Dohn, R.H. Carnahan, M.A. Davis, N.A. Lobdell, J. Settleman, and A.B. Reynolds. 2006. p120-catenin and p190RhoGAP regulate cell-cell adhesion by coordinating antagonism between Rac and Rho. *Cell.* 127:1027–1039. doi:10.1016/j.cell.2006.09.046

Wu, J., D.J. Mariner, M.A. Thoreson, and A.B. Reynolds. 1998. Production and characterization of monoclonal antibodies to the catenin p120ctn. *Hybridoma.* 17:175–183. doi:10.1089/hyb.1998.17.175

Xiao, K., D.F. Allison, K.M. Buckley, M.D. Kottke, P.A. Vincent, V. Faundez, and A.P. Kowalczyk. 2003. Cellular levels of p120 catenin function as a set point for cadherin expression levels in microvascular endothelial cells. *J. Cell Biol.* 163:535–545. doi:10.1083/jcb.200306001

Xu, C., M.S. Inokuma, J. Denham, K. Golds, P. Kundu, J.D. Gold, and M.K. Carpenter. 2001. Feeder-free growth of undifferentiated human embryonic stem cells. *Nat. Biotechnol.* 19:971–974. doi:10.1038/nbt1001-971

Xu, R.H., T.L. Sampsell-Barron, F. Gu, S. Root, R.M. Peck, G. Pan, J. Yu, J. Antosiewicz-Bourget, S. Tian, R. Stewart, and J.A. Thomson. 2008. NANOG is a direct target of TGFbeta/activin-mediated SMAD signaling in human ESCs. *Cell Stem Cell.* 3:196–206. doi:10.1016/j.stem.2008.07.001

Xu, Y., X. Zhu, H.S. Hahm, W. Wei, E. Hao, A. Hayek, and S. Ding. 2010. Revealing a core signaling regulatory mechanism for pluripotent stem cell survival and self-renewal by small molecules. *Proc. Natl. Acad. Sci. USA.* 107:8129–8134. doi:10.1073/pnas.1002024107

Yamada, S., S. Pokutta, F. Drees, W.I. Weis, and W.J. Nelson. 2005. Deconstructing the cadherin-catenin-actin complex. *Cell.* 123:889–901. doi:10.1016/j.cell.2005.09.020

Yu, J., M.A. Vodyanik, K. Smuga-Otto, J. Antosiewicz-Bourget, J.L. Frane, S. Tian, J. Nie, G.A. Jonsdottir, V. Ruotti, R. Stewart, I.I. Slukvin, and J.A. Thomson. 2007. Induced pluripotent stem cell lines derived from human somatic cells. *Science.* 318:1917–1920. doi:10.1126/science.1151526

Zhou, J., P. Su, L. Wang, J. Chen, M. Zimmermann, O. Genbacev, O. Afonja, M.C. Horne, T. Tanaka, E. Duan, et al. 2009. mTOR supports long-term self-renewal and suppresses mesoderm and endoderm activities of human embryonic stem cells. *Proc. Natl. Acad. Sci. USA.* 106:7840–7845. doi:10.1073/pnas.0901854106